

Theory of the dark state of polyenes and carotenoids

William Barford ^{*}*Department of Chemistry, Physical and Theoretical Chemistry Laboratory, University of Oxford, Oxford, OX1 3QZ, United Kingdom*

(Received 29 March 2022; accepted 22 June 2022; published 5 July 2022)

A theory is developed to describe the singlet dark state (usually labeled S_1 or $2A_g$) of polyenes and carotenoids. The properties of this state explain the nonemissive properties of linear polyenes, it is responsible for the photoprotection properties of carotenoids in light harvesting complexes, and because of its triplet-pair character, it is thought to be the cause of singlet fission in polyene-type systems. The theory described here assumes that in principle this state is a linear combination of singlet triplet-pairs and a singlet charge-transfer exciton. Crucially, these components only couple when the triplet pair occupies neighboring C-C dimers, such that an electron transfer between the triplets creates a nearest-neighbor singlet charge-transfer excitation. This local coupling stabilizes the $2A_g$ state and induces a nearest-neighbor attraction between the triplets. In addition, because of the electron-hole Coulomb attraction in the exciton, the increased probability that the electron-hole pair occupies neighboring dimers enhances the triplet-triplet attraction: the triplet pair is “slaved” to the singlet exciton. The theory also predicts that as the Coulomb interaction is increased, the $2A_g$ state evolves from a predominately charge-transfer exciton with a small component of triplet-pair character to a state predominately composed of a triplet pair with some exciton character. Above a critical Coulomb interaction there is a decoupling of the triplet-pair and exciton subspaces, such that the $2A_g$ state becomes entirely composed of unbound spin-correlated triplet pairs. The predictions of this theory of a triplet-pair binding energy in carotenoids of ca. 0.4 eV are consistent with density matrix renormalization group calculations of the Pariser-Parr-Pople (or extended Hubbard) model. It also predicts that the single-triplet component of the $2A_g$ state in carotenoids is ca. 50%.

DOI: [10.1103/PhysRevB.106.035201](https://doi.org/10.1103/PhysRevB.106.035201)

I. INTRODUCTION

The low-energy singlet dark state of polyenes, usually labeled S_1 or $2A_g$, has continued to fascinate researchers for over 50 years [1,2]. Its intriguing electronic properties are a consequence of electron-electron interactions and electron-nuclear coupling [3].

The triplet-pair or bimagnon character of the 2^1A_g state was first predicted theoretically by Schulten and Karplus in 1972 [2] and further elucidated by Tavan and Schulten in 1987 [4]. Using exciton-basis valence-bond theory and the Pariser-Parr-Pople (PPP) model, Chandross *et al.* [5] performed an extensive analysis of the electronic states of linear polyenes as function of Coulomb interaction and bond alternation. This latter work revealed the mixed triplet-pair and charge-transfer exciton character of the 2^1A_g state.

Via exact diagonalization of the Hubbard-Peierls model, Hayden and Mele [6] demonstrated the combined role of electronic interactions and electron-nuclear coupling in determining the four-soliton structure of this state for a chain of 16 C atoms. The four-soliton structure was further investigated for polyene chains of up to 100 C atoms by solving the Pariser-Parr-Pople-Peierls (PPPP) model using the density matrix renormalization group (DMRG) method [7,8]. Since a triplet excitation coupled to the nuclei creates a soliton-

antisoliton ($S\bar{S}$) pair, the four-soliton structure (i.e., a pair of soliton-antisoliton pairs) is further strong theoretical evidence of the triplet-pair character of the 2^1A_g state.

Solitons (S) and antisolitons (\bar{S}) are associated with domain walls in the bond alternation of linear polyenes [9,10]. They are also associated with spinons, the elementary excitations of a one-dimensional spin-1/2 quantum antiferromagnet [11,12]. A spinon is a charge-neutral, spin-1/2 object, while a triplet excitation is a bound spinon pair, which is recognized as an $S\bar{S}$ pair in the bond alternation. Thus the $S\bar{S}$ pair separation is a measure of the internal size of the triplet excitation. Similarly, the $S\bar{S}$ - $S\bar{S}$ separation is a measure of the triplet-triplet pair separation. Barford *et al.* [7,13] showed that in polyenes the $S\bar{S}$ separation converges to four C-C dimers, while the $S\bar{S}$ - $S\bar{S}$ separation converges to six dimers, indicating that the triplet pair is bound. Further numerical evidence that the triplet pair is bound in the 2^1A_g state was provided by Valentine *et al.* [13], who showed that its energy converges to a value of 0.3 eV lower than the energy of a pair of free triplets.

In the other limit of weak electronic correlations, as in light-emitting polymers, the $2^1A_g^-$ state is predominately a charge-transfer exciton [5]. The electron-hole wave function of this state has odd parity (i.e., the wave function is odd under an exchange of the electron and hole), and it lies higher in energy than the optically allowed $1^1B_u^+$ state (which is usually labeled S_2 in polyenes) whose electron-hole wave function has even parity.

^{*}william.barford@chem.ox.ac.uk

The reversal of energies of the $1^1B_u^+$ and $2^1A_g^-$ states in polyenes is partly a consequence of electronic interactions [5,14–16]. As explained later, electronic interactions simultaneously reduce the excitation energy of the lowest covalent triplet state and increase the excitation energy of ionic singlet states, which implies that for large enough interactions a triplet-pair state will have a lower energy than a singlet ionic state. The triplet-pair state is further stabilized relative to the ionic state, as electron-nuclear relaxation is enhanced in covalent states.

The energetic reversal of the bright (S_2) and dark (S_1) states has various photophysical consequences. For example, it explains the nonemissive properties of linear polyenes, it is responsible for the photoprotection properties of carotenoids in light-harvesting complexes, and, because of its triplet-pair character, it is thought to be the cause of singlet fission in polyene-type systems [17–21]. The electronic states of carotenoids are reviewed in Refs. [22–24], while Refs. [25–27] report on recent high-level *ab initio* calculations of these states.

As already noted, the 2^1A_g state of polyenes has been extensively studied via DMRG calculations of the PPPP model. As well as the four-soliton structure, triplet overlaps and spin-spin correlation functions also reveal its triplet-pair character [13]. Using a suitable exciton creation operator [28], Valentine *et al.* [13] also investigated the excitonic component of this state. Figure 8 of Ref. [13] illustrates the odd-parity charge-transfer exciton wave-function characteristic of the 2^1A_g state of more weakly correlated polymers.

Thus we can conclude that the 2^1A_g state is a linear combination of a singlet triplet-pair and an odd-parity charge-transfer exciton. This suggests that the mixing of the triplet-pair and charge-transfer exciton subspaces both stabilize the 2^1A_g state and cause the strong triplet-triplet attraction. This stabilization is an additional cause of the $1^1B_u/2^1A_g$ energy reversal in polyenes. The theory presented in this paper will explain this property.

The $2^1A_g^-$ state is the lowest energy member of a family of states with the same elementary excitations but with different pseudomomentum quantum numbers (i.e., $2^1A_g^-, 1^1B_u^-, 3^1A_g^-, \dots$), which, for convenience, we label as the “ $2A_g$ family.” Irrespective of their even or odd symmetry under a twofold rotation, these states are all optically dark. The singlet triplet-pair component of the $2A_g$ family is optically dark for two reasons. First, it is composed of a pair of electronic excitations, and since the dipole operator is a one-electron operator, the transition dipole moment with the ground state vanishes. Second, each electronic excitation is a triplet, and since the dipole operator commutes with total spin, the transition dipole moment with the singlet ground state again vanishes. The exciton component of the $2A_g$ family is also optically dark, because its electron-hole wave function has odd parity and thus its transition dipole moment with the ground state vanishes [3].

In this paper we describe an effective low-energy model of the $2A_g$ family of states in conjugated polyenes that provides a simple, physical explanation of triplet-pair binding. There are two key approximations in the model. First, it assumes that polyene chains are comprised of weakly interacting ethylene dimers. This implies that the ground state is composed of a

product of singlet dimer states. Second, it assumes a reduced basis for the excited states, composed of singlet triplet-pair excitations and odd-parity singlet electron-hole excitations.

Crucially, the theory predicts that when a pair of triplets occupy neighboring dimers, an electron transfer between the dimers connects the pair of triplets to the odd-parity charge-transfer exciton. This local coupling stabilizes the $2A_g$ state and induces a nearest-neighbor attraction between the triplets. In addition, because of the electron-hole attraction in the exciton, the increased probability that the electron-hole pair occupies neighboring dimers enhances the triplet-triplet attraction: the triplet pair is “slaved” to the exciton. The theory also predicts that as the Coulomb interaction increases, the exciton becomes energetically less stable relative to the triplet pair, causing a decoupling of the triplet-pair and exciton subspaces. This decoupling has been observed in computational studies of the PPPP model [3]. Above this critical Coulomb interaction, the triplet pairs unbind and the $2A_g$ state is entirely composed of spin-correlated triplet pairs.

Triplet-pair interactions within a dimerized antiferromagnetic chain have been investigated in Refs. [12,29,30], while stabilization of the $2A_g$ state via configuration interactions was also discussed in Ref. [31].

The next section describes the model where the reduced basis of pairs of intradimer and charge-transfer triplets, and singlet odd-parity electron-hole excitations are introduced. The predictions of the model for linear carotenoids and polyenes are described in Sec. III, while Sec. IV concludes the paper. Our reduced-basis model makes predictions consistent with higher-level DMRG calculations. However, additional physical insight into the character of the $2A_g$ state, the origin of triplet-pair binding, and the unbinding transition can be better understood via a minimal model of only intradimer triplet pairs and singlet electron-hole excitations. The predictions of this minimal model are described in Appendix B.

II. MODEL

A. Pariser-Parr-Pople model of π -conjugated polymers

Our starting point for the derivation of a low-energy effective model for the $2A_g$ state is the Pariser-Parr-Pople (PPP) model of π -conjugated polymers. This model is defined as

$$\begin{aligned} \hat{H}_{\text{PPP}} = & - \sum_{m\sigma} t_m (\hat{c}_{m\sigma}^\dagger \hat{c}_{m+1\sigma} + \hat{c}_{m+1\sigma}^\dagger \hat{c}_{m\sigma}) \\ & + U \sum_m \left(\hat{N}_{m\uparrow} - \frac{1}{2} \right) \left(\hat{N}_{m\downarrow} - \frac{1}{2} \right) \\ & + \sum_m \sum_{n \geq 1} V_n (\hat{N}_m - 1) (\hat{N}_{m+n} - 1), \end{aligned} \quad (1)$$

where $\hat{c}_{m\sigma}^\dagger$ ($\hat{c}_{m\sigma}$) creates (destroys) an electron with spin σ in the p_z orbital of carbon atom m . $\hat{N}_{m\sigma}$ is the corresponding number operator, and $\hat{N}_m = \sum_\sigma \hat{N}_{m\sigma}$. Assuming periodic bond alternation, the nearest-neighbor electron-transfer integral is

$$t_m = t_0 [1 + (-1)^m \delta], \quad (2)$$

where δ is the bond alternation parameter. For convenience, we define $t_d = t_0(1 + \delta)$ and $t_s = t_0(1 - \delta)$ as the

(a) $|\text{GS}\rangle = \alpha|1\rangle + \beta|2\rangle$

(b) $|\text{T}\rangle = \begin{bmatrix} \uparrow & \uparrow \\ \phi_1 & \phi_2 \end{bmatrix} \equiv \begin{bmatrix} \psi_- \uparrow \\ \psi_+ \uparrow \end{bmatrix}$

(c) $|\text{S}\rangle = \frac{1}{\sqrt{2}} \left\{ \begin{bmatrix} \uparrow\downarrow & \\ 1 & 2 \end{bmatrix} - \begin{bmatrix} & \uparrow\downarrow \\ 1 & 2 \end{bmatrix} \right\}$
 $\equiv \frac{1}{\sqrt{2}} \left\{ \begin{bmatrix} - & \uparrow \\ + & \downarrow \end{bmatrix} - \begin{bmatrix} \downarrow & \\ \uparrow & \end{bmatrix} \right\}$

(d) $|\text{X}\rangle = \beta|1\rangle - \alpha|2\rangle$

(e) $|1\rangle = \frac{1}{\sqrt{2}} \left\{ \begin{bmatrix} \uparrow & \downarrow \\ 1 & 2 \end{bmatrix} - \begin{bmatrix} \downarrow & \uparrow \\ 1 & 2 \end{bmatrix} \right\}$
 $|2\rangle = \frac{1}{\sqrt{2}} \left\{ \begin{bmatrix} \uparrow\downarrow & \\ 1 & 2 \end{bmatrix} + \begin{bmatrix} & \uparrow\downarrow \\ 1 & 2 \end{bmatrix} \right\}$

FIG. 1. The four electronic eigenstates of the two-electron ethylene dimer: (a) $|\text{GS}\rangle$, (b) $|\text{T}\rangle$, (c) $|\text{S}\rangle$, and (d) $|\text{X}\rangle$. (e) The basis states $|1\rangle$ (covalent) and $|2\rangle$ (ionic). The eigenstate energies, and α and β , are given in Appendix A. Also shown in (b) and (c) is the equivalence between the dimer atomic-orbital representation (i.e., ϕ_1 and ϕ_2) and molecular-orbital representation (i.e., $\psi_{\pm} = (\phi_1 \pm \phi_2)/\sqrt{2}$).

double- and single-bond transfer integrals, respectively. The Coulomb interaction is represented by the Ohno potential, i.e.,

$$V_n = \frac{U}{[1 + (U\epsilon r_n/14.397)^2]^{1/2}}, \quad (3)$$

where U is in eV, the separation between atoms m and $m+n$, r_n , is in Å, and ϵ is the relative permittivity.

Typical parameter values for π -conjugated polymers [32] are $U = 8$ eV, $\epsilon = 2$, and $t_0 = 2.4$ eV. In addition, for polyenes, $\delta = 1/12$, so that $t_d = 2.6$ eV and $t_s = 2.2$ eV.

B. Effective model of the $2A_g$ state

The model assumes that carotenoids and polyenes are linear chains of coupled ethylene dimers, where a dimer is

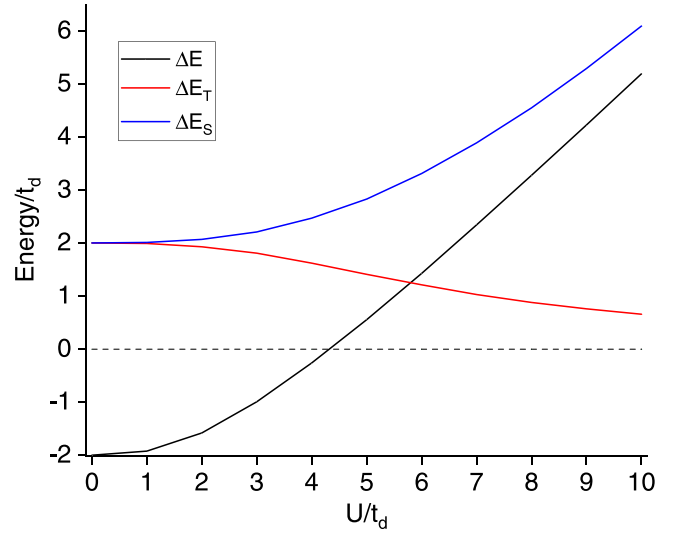


FIG. 2. The ethylene dimer triplet, ΔE_T , and singlet, ΔE_S , excitation energies as a function of U/t_d . Also shown for neighboring dimers is the energy of the charge-transfer exciton relative to a pair of triplets, $\Delta E = [(E_{\text{EX}} - \tilde{V}_1) - E_{\text{TT}}]$, where $-\tilde{V}_1$ is the nearest-neighbor electron-hole interaction.

composed of two carbon atoms each with a single p_z orbital. The four electronic states of a dimer with two π electrons are illustrated in Fig. 1. The singlet ground state, $|\text{GS}\rangle = \alpha|1\rangle + \beta|2\rangle$, is a linear combination of covalent and ionic states (i.e., $|1\rangle$ and $|2\rangle$). As shown by Eq. (A6), for noninteracting electrons (i.e., $U = 0$), $\alpha = \beta = 1/\sqrt{2}$, while as $U/t_d \rightarrow \infty$, $\alpha \rightarrow 1$. For realistic polyene parameters, $\alpha \sim \sqrt{2/3}$.

In general, the lowest energy excitation is the covalent triplet state, $|\text{T}\rangle$, while the lowest singlet excitation is the ionic state, $|\text{S}\rangle$. The excitation energies of these two states as a function of U/t_d are illustrated in Fig. 2. In the non-interacting limit these excitation energies are degenerate at $2t_d$. However, as U increases, the ground state becomes more covalent and for large U the triplet excitation energy decreases as $4t_d^2/(U - V_1)$. In contrast, the singlet excitation energy increases as $(U - V_1)$. Appendix A discusses the dimer solutions in more detail (also see Refs. [5,15]).

The next two sections introduce the singlet triplet-pair and electron-pair bases for polyene chains, which are used as an approximate representation for the $2A_g$ state. This approach is in the spirit, albeit an approximation as it is an incomplete basis, of the exciton-basis valence-bond theory discussed in Ref. [5].

1. Singlet triplet-pair basis

We now make the assumption that the ground state of polyenes can be approximated as a product of dimer ground states, i.e., $|\text{GS}\rangle = \Pi_i |\text{GS}; i\rangle$, where the product is over all dimers, and $|\text{GS}; i\rangle$ is the ground state for dimer i , defined in Eq. (A5).

The lowest-energy triplet excitation from the polyene ground state then corresponds to a triplet excitation on a single dimer (i.e., $|\text{T}\rangle$, as shown in Fig. 1). Its excitation energy is

$$E_T = V_1 - E_{\text{GS}}^{\text{dimer}}, \quad (4)$$

$$|CT, 1, i\rangle = \frac{1}{\sqrt{2}} \left[\left\{ \begin{array}{c} \uparrow \\ \downarrow \end{array} \right\}_i - \left\{ \begin{array}{c} \uparrow \\ \uparrow \end{array} \right\}_{i+1} \right] - \left[\left\{ \begin{array}{c} \uparrow \\ \uparrow \end{array} \right\}_i - \left\{ \begin{array}{c} \uparrow \\ \downarrow \end{array} \right\}_{i+1} \right]$$

FIG. 3. Molecular orbital representation of the symmetrized even-parity nearest-neighbor charge-transfer triplet, $|CT, M_S = 1; i\rangle$.

where E_{GS}^{dimer} is defined in Eq. (A2). We denote this state as $|T, M_S; i\rangle$, where M_S is the spin projection (i.e., 1, 0, or -1) and i labels the dimer. The triplet on dimer i , $|T, M_S; i\rangle$, can hop to neighboring dimers, $|T, M_S; i \pm 1\rangle$, via a charge-transfer triplet state higher in energy. This symmetrized even-parity nearest-neighbor charge-transfer triplet, denoted as $|CT, M_S; i\rangle$, is illustrated in Fig. 3. Its excitation energy is

$$E_{CT} = (U + 2V_1 - 2t_d) - 2E_{GS}^{\text{dimer}} - \tilde{V}_1, \quad (5)$$

where \tilde{V}_1 [defined in Eq. (18)] is the energy gained by the Coulomb interaction between the electron and hole. The matrix element coupling these triplets is

$$t_{TT} = \sqrt{2} \left(\frac{t_s}{2} \right) = t_s / \sqrt{2}, \quad (6)$$

where the factor of $1/2$ in the first term on the right-hand side arises from the overlap of the molecular orbitals on neighboring dimers and the factor of $\sqrt{2}$ arises because $|T; i\rangle$ is connected to $|CT; i\rangle$ and $|CT; i-1\rangle$ by an electron transfer between lowest unoccupied molecular orbitals (LUMOs) and a hole transfer between highest occupied molecular orbitals (HOMOs).

The lowest energy triplet-pair excitation corresponds to $|T\rangle$ excitations on separate dimers, i and j . A pair of such spin-correlated triplets can form an overall singlet, triplet, or

quintet state. Here we are concerned with the singlet triplet-pair state, expressed as

$$|TT; i, j\rangle = \frac{1}{\sqrt{3}} (|T, 1; i\rangle |T, -1; j\rangle - |T, 0; i\rangle |T, 0; j\rangle + |T, -1; i\rangle |T, 1; j\rangle), \quad (7)$$

where $1 \leq i \leq N$ and $1 \leq j \leq N$, and the constraints $i \neq j$ mean that the triplets cannot occupy the same dimer. This state is illustrated schematically in Fig. 4.

The PPP Hamiltonian connects each $|T; i\rangle$ component of $|TT; i, j\rangle$ to a charge-transfer triplet, $|CT; i-1\rangle$ and $-|CT; i\rangle$. Thus our triplet-pair basis includes a pair of $|T\rangle$ and $|CT\rangle$ excitations, i.e.,

$$|TCT; i, j\rangle = \frac{1}{\sqrt{3}} (|T, 1; i\rangle |CT, -1; j\rangle - |T, 0; i\rangle |CT, 0; j\rangle + |T, -1; i\rangle |CT, 1; j\rangle), \quad (8)$$

where $1 \leq i \leq N$ and $1 \leq j \leq N-1$.

Similarly, the PPP Hamiltonian connects each $|T; i\rangle$ component of $|TCT; i, j\rangle$ to another charge-transfer triplet. Our basis, therefore, also consists of pairs of triplet charge-transfer excitations,

$$|CTCT; i, j\rangle = \frac{1}{\sqrt{3}} (|CT, 1; i\rangle |CT, -1; j\rangle - |CT, 0; i\rangle |CT, 0; j\rangle + |CT, -1; i\rangle |CT, 1; j\rangle), \quad (9)$$

where $1 \leq i \leq N-1$ and $1 \leq j \leq N-1$.

$$|TT; i, j\rangle = \frac{1}{\sqrt{3}} \left[\left\{ \begin{array}{cc} \uparrow & \uparrow \\ 1 & 2 \end{array} \right\} \text{---} \text{---} \begin{array}{cc} \downarrow & \downarrow \\ 1 & 2 \end{array} \right\} - \left\{ \begin{array}{cc} \uparrow & \uparrow \\ 1 & 2 \end{array} \right\} \text{---} \text{---} \begin{array}{cc} \downarrow & \downarrow \\ 1 & 2 \end{array} \right\} \right]$$

$$- \left\{ \frac{1}{\sqrt{2}} \left\{ \begin{array}{cc} \uparrow & \downarrow \\ 1 & 2 \end{array} \right\} + \begin{array}{cc} \downarrow & \uparrow \\ 1 & 2 \end{array} \right\} \text{---} \text{---} \frac{1}{\sqrt{2}} \left\{ \begin{array}{cc} \uparrow & \downarrow \\ 1 & 2 \end{array} \right\} + \begin{array}{cc} \downarrow & \uparrow \\ 1 & 2 \end{array} \right\} \right\} + \left\{ \begin{array}{cc} \downarrow & \downarrow \\ 1 & 2 \end{array} \right\} \text{---} \text{---} \begin{array}{cc} \uparrow & \uparrow \\ 1 & 2 \end{array} \right\} \right]$$

FIG. 4. Atomic orbital representation of the singlet triplet-pair basis state, $|TT; i, j\rangle = (|T, 1; i\rangle |T, -1; j\rangle - |T, 0; i\rangle |T, 0; j\rangle + |T, -1; i\rangle |T, 1; j\rangle) / \sqrt{3}$, with triplet excitations on dimers i and j . The dashed lines --- represent $(j-i-1)$ dimers in their singlet ground state. When $j = i+1$, the state labeled $*$ is connected to the state labeled \times in Fig. 5 via an electron transfer across the single bond.

$$\begin{aligned}
\text{(a)} \quad |EX; i, j\rangle &= \frac{1}{2} \left[\begin{aligned} &\left\{ \begin{array}{c} \begin{array}{|c|} \hline \uparrow \\ \hline \end{array} \\ \begin{array}{|c|} \hline \uparrow\downarrow \\ \hline \end{array} \end{array} \text{---} \begin{array}{c} \begin{array}{|c|} \hline \text{---} \\ \hline \end{array} \\ \begin{array}{|c|} \hline \downarrow \\ \hline \end{array} \end{array} \right\} - \left\{ \begin{array}{c} \begin{array}{|c|} \hline \downarrow \\ \hline \end{array} \\ \begin{array}{|c|} \hline \uparrow\downarrow \\ \hline \end{array} \end{array} \text{---} \begin{array}{c} \begin{array}{|c|} \hline \text{---} \\ \hline \end{array} \\ \begin{array}{|c|} \hline \uparrow \\ \hline \end{array} \end{array} \right\} \\ &+ \left\{ \begin{array}{c} \begin{array}{|c|} \hline \text{---} \\ \hline \end{array} \\ \begin{array}{|c|} \hline \downarrow \\ \hline \end{array} \end{array} \text{---} \begin{array}{c} \begin{array}{|c|} \hline \uparrow \\ \hline \end{array} \\ \begin{array}{|c|} \hline \uparrow\downarrow \\ \hline \end{array} \end{array} \right\} - \left\{ \begin{array}{c} \begin{array}{|c|} \hline \text{---} \\ \hline \end{array} \\ \begin{array}{|c|} \hline \uparrow \\ \hline \end{array} \end{array} \text{---} \begin{array}{c} \begin{array}{|c|} \hline \downarrow \\ \hline \end{array} \\ \begin{array}{|c|} \hline \uparrow\downarrow \\ \hline \end{array} \end{array} \right\} \end{aligned} \right] \\
\text{(b)} \quad \begin{array}{c} \begin{array}{|c|} \hline \text{---} \\ \hline \end{array} \\ \begin{array}{|c|} \hline \uparrow \\ \hline \end{array} \end{array} \equiv \frac{1}{\sqrt{2}} \left\{ \begin{array}{c} \begin{array}{|c|} \hline \uparrow \\ \hline \end{array} \\ \begin{array}{|c|} \hline \text{---} \\ \hline \end{array} \end{array} \begin{array}{c} \begin{array}{|c|} \hline \text{---} \\ \hline \end{array} \\ \begin{array}{|c|} \hline \uparrow \\ \hline \end{array} \end{array} \right\} \\
\begin{array}{c} \begin{array}{|c|} \hline \uparrow \\ \hline \end{array} \\ \begin{array}{|c|} \hline \uparrow\downarrow \\ \hline \end{array} \end{array} \equiv \frac{1}{\sqrt{2}} \left\{ \begin{array}{c} \begin{array}{|c|} \hline \uparrow\downarrow \\ \hline \end{array} \\ \begin{array}{|c|} \hline \text{---} \\ \hline \end{array} \end{array} \begin{array}{c} \begin{array}{|c|} \hline \uparrow \\ \hline \end{array} \\ \begin{array}{|c|} \hline \uparrow\downarrow \\ \hline \end{array} \end{array} \right\}
\end{aligned}$$

FIG. 5. (a) Molecular-orbital representation of the singlet charge-transfer exciton-basis state, $|EX; i, j\rangle$, with electron-hole excitations on dimers i and j . (b) The equivalence between the dimer molecular-orbital and atomic-orbital representations. When $j = i + 1$, the state labeled \times is connected to the state labeled $*$ in Fig. 4 via an electron transfer across the single bond.

The Hamiltonian that describes this singlet triplet-pair subspace is

$$\begin{aligned}
\hat{H}_{\text{triplet-pair}} &= \frac{E_{\text{TT}}}{2} \sum_{ij} |\text{TT}; i, j\rangle \langle \text{TT}; i, j| \\
&+ \frac{E_{\text{TCT}}}{2} \sum_{ij} |\text{TCT}; i, j\rangle \langle \text{TCT}; i, j| \\
&+ \frac{E_{\text{CTCT}}}{2} \sum_{ij} |\text{CTCT}; i, j\rangle \langle \text{CTCT}; i, j| \\
&+ t_{\text{TT}} \sum_{ij} (|\text{TCT}; i, j-1\rangle \langle \text{TT}; i, j| + \text{H.C.}) \\
&- t_{\text{TT}} \sum_{ij} (|\text{TCT}; i, j\rangle \langle \text{TT}; i, j| + \text{H.C.}) \\
&+ t_{\text{TT}} \sum_{ij} (|\text{CTCT}; i-1, j\rangle \langle \text{TCT}; i, j| + \text{H.C.}) \\
&- t_{\text{TT}} \sum_{ij} (|\text{CTCT}; i, j\rangle \langle \text{TCT}; i, j| + \text{H.C.}) \quad (10)
\end{aligned}$$

The first four terms on the right-hand side describe the energy to excite a pair of triplets on different dimers i and j , where

$$E_{\text{TT}} = 2E_{\text{T}}, \quad (11)$$

$$E_{\text{TCT}} = E_{\text{T}} + E_{\text{CT}}, \quad (12)$$

$$E_{\text{CTCT}} = 2E_{\text{CT}}, \quad (13)$$

$$E_{\text{TT}} < E_{\text{TCT}} < E_{\text{CTCT}}, \quad (14)$$

and the factors of $1/2$ account for double counting. The remaining terms describe the triplet transfer processes described above, where the constraints of hard-core repulsion are assumed.

2. Singlet charge-transfer exciton basis

The second type of excitations from the ground state are singlet electron-hole excitations. The dimer state $|S\rangle$ shown in Fig. 1 is the basis state for the tightly bound Frenkel exciton of conjugated polymers [3]. Because of its even electron-hole parity, however, this state cannot couple with a singlet triplet-pair state. For an electron-hole excitation to couple to a triplet-pair state it must have odd electron-hole parity, which implies a charge-transfer state as illustrated in Fig. 5. The electron in the antibonding ψ_- dimer orbital and a hole in the bonding ψ_+ dimer orbital hop between neighboring dimers via the transfer integral

$$t_{\text{EX}} = t_s/2, \quad (15)$$

where the factor of $1/2$ arises from the overlap of neighboring dimer orbitals.

The Hamiltonian that describes the odd-parity singlet-exciton subspace is

$$\hat{H}_{\text{EX}} = \frac{1}{2} \sum_{ij} (E_{\text{EX}} - \tilde{V}_{(j-i)}) |\text{EX}; i, j\rangle \langle \text{EX}; i, j| + t_{\text{EX}} \sum_{ij} (|\text{EX}; i \pm 1, j\rangle \langle \text{EX}; i, j| + \text{H.c.}). \quad (16)$$

The first term on the right-hand side describes the energy to excite an electron-hole pair on different dimers i and j , where

$$E_{\text{EX}} = (U + 2V_1 - 2t_d) - 2E_{\text{GS}}^{\text{dimer}}. \quad (17)$$

In addition, there is a Coulomb attraction between the electron-hole pair $\ell = (j - i)$ dimers apart, given by

$$\tilde{V}_\ell = (V_{2\ell-1} + 2V_{2\ell} + V_{2\ell+1})/4. \quad (18)$$

The final term describes the (symmetrized) motion of the electron or hole between neighboring dimers.

As described in Ref. [33], in the continuum limit for a $1/r$ Coulomb interaction there is a Rydberg series of odd-parity bound electron-hole pairs. The $2A_g$ charge-transfer exciton state is the lowest energy member of this series [34]. The even-parity excitons alternate in energy with the odd-parity excitons, while the lowest even-parity (Frenkel) exciton is split off from the Rydberg series [3,33].

The relative energies of the triplet-pair and electron-hole pair for neighboring dimers is illustrated in Fig. 2. In the noninteracting limit a single triplet is degenerate with a singlet electron-hole excitation, so $\Delta E = (E_{\text{EX}} - E_{\text{TT}})$ is negative. However, as we have seen, as U increases the triplet energy decreases while the electron-hole energy increases, causing a reversal of energies at $U \sim 4t_d$. It is this property of covalent and ionic states which partially stabilizes the $2^1A_g^-$ state relative to the optically active $1^1B_u^+$ Frenkel exciton state in polyenes.

3. Triplet-pair and charge-transfer exciton coupling

We now consider the coupling between the singlet triplet-pair and the odd-parity singlet-exciton subspaces. As described in Sec. II B 1, the PPP Hamiltonian connects an isolated intradimer triplet, $|\text{T}\rangle$, to a charge-transfer triplet, $|\text{CT}\rangle$. However, for the special case that a pair of intradimer triplet excitations occupy neighboring dimers, i.e., $|\text{TT}; i, i+1\rangle$, an electron transfer across the single bond between them creates a nearest-neighbor electron-hole pair, i.e., $|\text{EX}; i, i+1\rangle$. This may be understood by examining the basis states labeled \times in Fig. 4 and \times in Fig. 5. By inspection of \times in Fig. 4, we observe that a transfer of the down electron on site 1 of dimer $j = i+1$ to site 2 of dimer i creates a component of the basis state \times in Fig. 5.

The Hamiltonian describing this process is

$$\hat{H}_{\text{EX-TT}} = -V_{\text{EX-TT}} \sum_i (|\text{EX}; i, i+1\rangle \langle \text{TT}; i, i+1| + \text{H.c.}), \quad (19)$$

where

$$V_{\text{EX-TT}} = \sqrt{3}t_s/2. \quad (20)$$

Since this term only connects a nearest-neighbor triplet pair with a nearest-neighbor electron-hole pair, it results in an attraction between the triplet pair and an additional attraction above the Coulomb interaction for the electron-hole pair.

4. The $2A_g$ state

We express an eigenstate of the full effective Hamiltonian,

$$\hat{H} = \hat{H}_{\text{triplet-pair}} + \hat{H}_{\text{EX}} + \hat{H}_{\text{EX-TT}}, \quad (21)$$

as

$$|\Psi\rangle = \sum_{ij} \Psi_{ij}^{\text{TT}} |\text{TT}; i, j\rangle + \Psi_{ij}^{\text{TCT}} |\text{TCT}; i, j\rangle + \Psi_{ij}^{\text{CTCT}} |\text{CTCT}; i, j\rangle + \Psi_{ij}^{\text{EX}} |\text{EX}; i, j\rangle. \quad (22)$$

Since this is a linear combination of basis states from the triplet-pair and singlet-exciton sub-bases and not formed via a direct product of the sub-bases, the interaction $V_{\text{EX-TT}}$ does not correlate (or entangle) the triplet-pair and singlet exciton. Instead, it stabilizes the linear combination and causes a triplet-triplet attraction.

III. RESULTS AND DISCUSSION

We now describe the solutions of the effective model of the $2A_g$ state for linear carotenoids and polyenes. The model parameters are derived from the underlying PPP model, Eq. (1). In this case, as shown by Eq. (11), Eq. (15), Eq. (17), Eq. (18), and Eq. (20), the model parameters are determined by the Coulomb interaction U and the bond dimerization δ .

We define two energy gaps. First, the stabilization energy gained by the $2A_g$ state caused by the coupling of the triplet-pair and singlet-exciton subspaces, i.e.,

$$\Delta_{2A_g} = \langle \hat{H}_{\text{triplet-pair}} + \hat{H}_{\text{EX}} \rangle - \langle \hat{H} \rangle. \quad (23)$$

Second, the triplet-pair binding energy, defined as the energy gap between the band of free (spin-correlated) triplet pairs and the stabilized $2A_g$ state, i.e.,

$$\Delta_{\text{triplet-pair}} = \langle \hat{H}_{\text{triplet-pair}} \rangle - \langle \hat{H} \rangle. \quad (24)$$

The state will be characterized by its triplet-pair weight, i.e.,

$$P_{\text{triplet-pair}} = \sum_{ij} |\Psi_{ij}^{\text{TT}}|^2 + |\Psi_{ij}^{\text{TCT}}|^2 + |\Psi_{ij}^{\text{CTCT}}|^2, \quad (25)$$

and the mean triplet-pair separation (in monomer units), i.e.,

$$L_{\text{triplet-pair}} = \frac{\sum_{ij} |j-i| (|\Psi_{ij}^{\text{TT}}|^2 + |\Psi_{ij}^{\text{TCT}}|^2 + |\Psi_{ij}^{\text{CTCT}}|^2)}{P_{\text{triplet-pair}}}. \quad (26)$$

Note that the *singlet*-triplet weight is

$$P_{\text{triplet}} = 2P_{\text{triplet-pair}}/(1 + P_{\text{triplet-pair}}). \quad (27)$$

We first consider the predictions of the model as a function of chain length for realistic PPP parameters, i.e., $U = 8$ eV, $\epsilon = 2$, $t_0 = 2.4$ eV, and $\delta = 1/12$. Figure 6 shows that for these parameters the triplet pair is bound with a binding energy that decreases with chain length and converges to ca. 3.5 eV. These predictions are in good agreement with DMRG calculations of the PPP model [13]. The triplet-pair weight

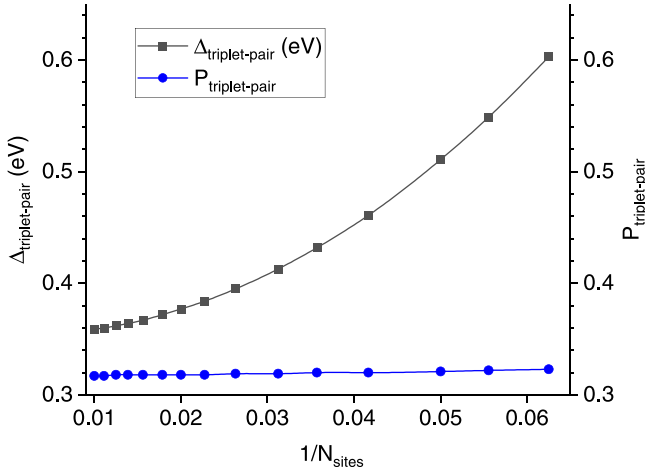


FIG. 6. The triplet-pair binding energy, $\Delta_{\text{triplet-pair}}$, and overall contribution to the $2A_g$ state, $P_{\text{triplet-pair}}$, as a function of the inverse number of C sites, N_{sites} . $U = 8$ eV, $\epsilon = 2$, $t_0 = 2.4$ eV, and $\delta = 1/12$.

remains almost constant as a function of chain length at ca. 33% (implying a single-triplet weight [via Eq. (27)] of ca. 50%). The triplet-triplet separation also remains constant at ca. 1.3 dimers.

We next explore the predictions of the model as a function of the Coulomb interaction U for a linear chain of 40 C sites (or 20 double bonds). These results are shown in Fig. 7. As expected from the discussion in Sec. II B, for large enough U , i.e., $U \geq 7.2$ eV, the triplet pairs are more stable than the singlet charge-transfer exciton, and $\Delta_{\text{triplet-pair}} = \Delta_{2A_g}$. As U is further increased, the triplet-pair weight and separation in-

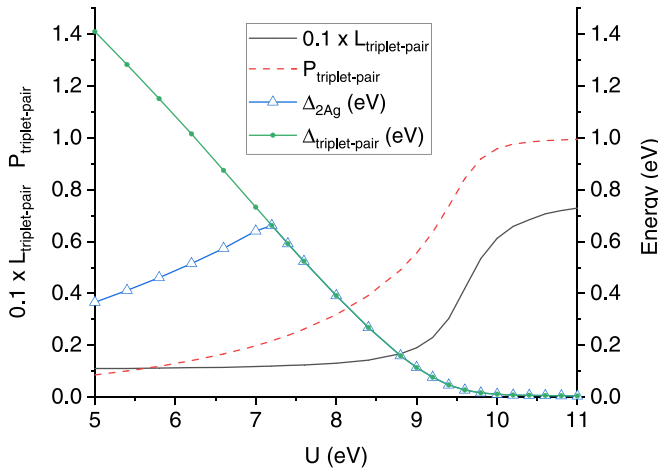


FIG. 7. Results as a function of the Coulomb repulsion U for a linear polyene of 40 C atoms using effective model parameters derived from the PPP model (see Sec. II B). Δ_{2A_g} , Eq. (23), is the stabilization energy of the $2A_g$ state caused by the coupling of the triplet-pair and electron-hole pair; $\Delta_{\text{triplet-pair}}$, Eq. (24), is the triplet-pair binding energy; $L_{\text{triplet-pair}}$, Eq. (25), is the mean triplet-pair separation (scaled by 0.1 and in units of dimers); and $P_{\text{triplet-pair}}$, Eq. (26), is the triplet-pair weight. For $U \geq 7.2$ eV, the triplet pairs are more stable than the singlet charge-transfer exciton. The triplet-pair and singlet charge-transfer exciton subspaces decouple for $U \gtrsim 11$ eV, and the triplets unbind.

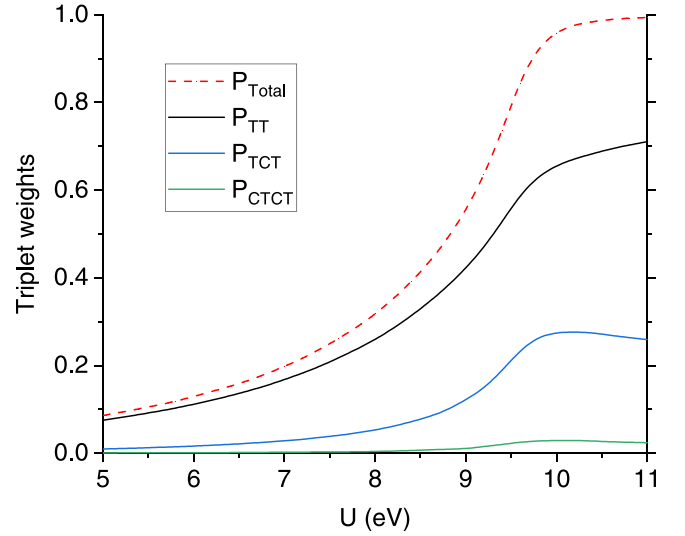


FIG. 8. Triplet-pair weights of the $2A_g$ state as a function of the Coulomb interaction, U .

crease while the binding energy decreases. For $U \gtrsim 11$ eV, the triplet-pair and singlet-exciton subspaces decouple, implying a triplet-pair unbinding transition and that the $2A_g$ state is entirely composed of triplet pairs. This prediction of decoupling above a critical U is consistent with DMRG calculations of the PPP model, as shown in Fig. 7.8 of Ref. [3].

Conversely, as U is decreased from $U = 7.2$ eV, the singlet charge-transfer exciton is more stable than the triplet pairs, and Δ_{2A_g} and the triplet-pair weight decrease. Unlike the large- U limit, however, there is no decoupling of the triplet-pair and singlet-exciton subspaces, although the triplet-pair weight is less than 1% for $U \lesssim 2$ eV. Figure 8 illustrates the weights of the different triplet-pair components of the $2A_g$ state as a function of U . As expected from energetic considerations, the $|\text{TT}; i, j\rangle$ component dominates the triplet pair, with its contribution being ca. 80% when $U = 8$ eV.

In summary, the model calculations on linear polyenes show how the character of the $2A_g$ state and the triplet-pair binding energy varies with the Coulomb interaction. However, two key predictions of the theory, namely, that the triplet-pair binding is enhanced because the triplet pairs couple to a Coulombically bound singlet electron-hole pair and that there is decoupling of the triplet-pair and singlet-exciton subspaces (and hence triplet-pair unbinding) for large Coulomb interactions, is more clearly understood via a minimal model of the $2A_g$ state. This model and its predictions are described in Appendix B.

Finally, we explore the role of the bond alternation, δ , for a fixed $U = 8$ eV. The bond alternation is sometimes used as a proxy to describe the different electronic properties of non-emissive polyenes and light-emitting phenyl-based polymers [14]. Extrapolating the predictions of the PPP model with a polyene geometry between small and large δ is a proxy for extrapolating between polyenes and phenyl-based systems, because increasing δ decreases E_{EX} and hence stabilizes the singlet exciton. It also reduces t_{EX} , $|t_{\text{TT}}|$, and $V_{\text{TT-EX}}$. Thus, as shown in via Fig. 9, the triplet pairs are more stable than the

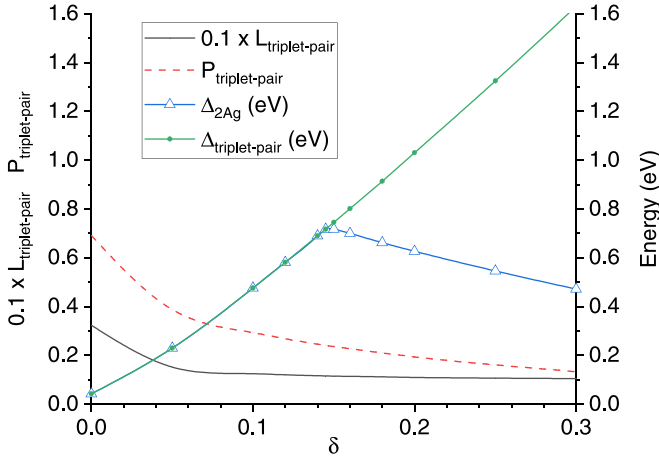


FIG. 9. Results as a function of the bond alternation δ for a linear chain of 40 C atoms using effective model parameters derived from the PPP model (see Sec. II B). The Coulomb repulsion, $U = 8$ eV. For $\delta \leq 0.1$ the triplet-pair state is more stable than the singlet exciton.

singlet exciton for $\delta \leq 0.1$. In this case there is no decoupling of the subspaces.

IV. CONCLUDING REMARKS

This paper has introduced a theory to describe the singlet dark state (i.e., S_1 or $2A_g$) of polyenes and carotenoids. The theory assumes that in principle this state is a linear combination of singlet triplet pairs and an odd-parity charge-transfer exciton. Crucially, these components only couple when a pair of intradimer triplets occupy neighboring dimers, such that an electron transfer between the triplets creates a nearest-neighbor charge-transfer excitation. This local coupling stabilizes the $2A_g$ state and induces a nearest-neighbor attraction between the triplets. In addition, as explained in Appendix B, because of the electron-hole attraction in the exciton, the increased probability that the electron-hole pair occupies neighboring dimers enhances the triplet-triplet attraction: the triplet pair is “slaved” to the charge-transfer exciton. The reduction of the $2A_g$ energy is an additional cause for the $1^1B_u/2^1A_g$ energy reversal in polyenes.

The theory also predicts that as the Coulomb interaction is increased, the $2A_g$ state evolves from a predominately odd-parity charge-transfer exciton with a small component of triplet-pair character to a state predominately composed of triplet pairs with some exciton character. Above a critical Coulomb interaction there is a decoupling of the triplet-pair and charge-transfer exciton subspaces such that the $2A_g$ state becomes entirely composed of an unbound spin-correlated triplet pair.

The predictions of this theory of a large triplet-pair binding energy in carotenoids of ca. 0.4 eV are consistent with DMRG [3,13] calculations of the PPP model. We also predict that the single-triplet component of the $2A_g$ state is ca. 50%. In addition, the theory provides a simple, physical explanation of the origin of triplet-triplet binding and a prediction of how the character of the $2A_g$ state varies with Coulomb repulsion and bond alternation.

As will be discussed in a forthcoming publication, the charge-transfer component of the $2A_g$ state explains the mechanism of internal conversion in carotenoids from the photoexcited state, S_2 or $1B_u$, to this state.

APPENDIX A: DIMER BASIS STATES

This Appendix summarizes the exact results of the PPP model for the eigenstates of the ethylene dimer illustrated in Fig. 1.

The triplet excitation energy is

$$\begin{aligned} \Delta E_T &= V_1 - E_{GS}^{\text{dimer}} \\ &\rightarrow 2t_d \text{ as } U/t_d \rightarrow 0 \\ &\rightarrow J_d \text{ as } U/t_d \rightarrow \infty, \end{aligned} \quad (\text{A1})$$

where $J_d = 4t_d^2/(U - V_1)$, the ground-state energy is

$$E_{GS}^{\text{dimer}} = (U + V_1)/2 - \epsilon, \quad (\text{A2})$$

and

$$\epsilon = \frac{1}{2}[(U - V_1)^2 + 16t_d^2]^{1/2}. \quad (\text{A3})$$

The lowest singlet excitation energy is

$$\begin{aligned} \Delta E_S &= U - E_{GS}^{\text{dimer}} \\ &\rightarrow 2t_d \text{ as } U/t_d \rightarrow 0 \\ &\rightarrow (U - V_1) + J_d \text{ as } U/t_d \rightarrow \infty. \end{aligned} \quad (\text{A4})$$

The ground state is

$$|GS\rangle = \alpha|1\rangle + \beta|2\rangle, \quad (\text{A5})$$

where the basis kets $|1\rangle$ and $|2\rangle$ are illustrated in Fig. 1, and

$$\begin{aligned} \alpha &= \frac{1}{2} \left(\frac{2\epsilon + (U - V_1)}{\epsilon} \right)^{1/2} \\ &\rightarrow \frac{1}{\sqrt{2}} \text{ as } U/t_d \rightarrow 0 \\ &\rightarrow 1 \text{ as } U/t_d \rightarrow \infty. \end{aligned} \quad (\text{A6})$$

Also, $\beta = (1 - \alpha^2)^{1/2}$.

APPENDIX B: A MINIMAL MODEL OF THE $2A_g$ STATE

In this Appendix we investigate a minimal, simplified model which provides an appealing description of the $2A_g$ state. In particular, it illustrates how the triplet-pair coupling to the Coulombically bound singlet electron-hole pair enhances the triplet-pair binding. It also shows that the decoupling of the triplet-pair and singlet-exciton subspaces (and concomitantly the triplet-pair unbinding) only occurs above and not below a critical Coulomb interaction.

The simplified model assumes that the triplet-pair basis is only spanned by the intradimer triplet pairs, i.e., $\{|TT; i, j\rangle\}$. As shown in Fig. 8, this is a reasonable assumption over most of the parameter regime, as the charge-transfer triplets are higher in energy and thus have a much smaller probability of contributing to the $2A_g$ state. Instead, the charge-transfer triplets now play the role of virtual states by which the intradimer triplets, $\{|T; i\rangle\}$, hop between dimers via a second-order process.

The triplet-pair Hamiltonian thus simplifies to

$$\hat{H}_{\text{triplet-pair}} = \frac{E_{\text{TT}}}{2} \sum_{ij} |\text{TT}; i, j\rangle \langle \text{TT}; i, j| + t_{\text{TT}} \sum_{ij} (|\text{TT}; i \pm 1, j\rangle \langle \text{TT}; i, j| + \text{H.c.}). \quad (\text{B1})$$

The superexchange transfer integral is

$$t_{\text{TT}} = -\frac{\alpha^2 t_s^2}{(E_{\text{CT}} - E_{\text{T}})}, \quad (\text{B2})$$

where α^2 [defined in Eq. (A6)] is the probability that the neighboring singlet dimer is in the covalent state labeled $|1\rangle$ in Fig. 1. \hat{H}_{EX} and $\hat{H}_{\text{EX-TT}}$ remain the same as before.

We start our investigation of the predictions of this model by considering arbitrary model parameters. We assume periodic boundary conditions for a system with 1000 monomers. In addition, we initially take the simplest limit of noninteracting electron-hole pairs, i.e., we set the Coulomb interaction $\tilde{V}_{(j-i)} = 0$ in Eq. (16). In this limit there is a symmetry between the triplet-pair and the electron-hole pair under the exchange $E_{\text{EX}} \leftrightarrow E_{\text{TT}}$ and $|t_{\text{EX}}| \leftrightarrow |t_{\text{TT}}|$. In the absence of the coupling, $V_{\text{EX-TT}}$, between the two subspaces the triplet pair forms a band of free triplet excitations (subject to a hard-core repulsion) centered at E_{TT} of width $8|t_{\text{TT}}|$. Likewise, there is a band of unbound electron-hole excitations centered at E_{EX} of width $8|t_{\text{EX}}|$.

Turning on the coupling, $V_{\text{EX-TT}}$, causes the nearest-neighbor triplet pair to mix with the nearest-neighbor electron-hole pair. At resonance, i.e., when $E_{\text{EX}} = E_{\text{TT}}$ and $|t_{\text{EX}}| = |t_{\text{TT}}|$, the mixing causes a nearest-neighbor attraction of $V_{\text{EX-TT}}$ for both the triplet and electron-hole pairs. This model then maps onto the well-known one-dimensional lattice model of spinless fermions interacting with a nearest-neighbor attraction, $V_{\text{EX-TT}}$, for which above a critical value of $V_{\text{EX-TT}}$ there is a single band of bound states. As shown in Refs. [35–37], the binding energy for the zero-momentum state is

$$E_{\text{BE}} = V_{\text{EX-TT}} + \frac{4t_{\text{TT}}^2}{V_{\text{EX-TT}}} - 4|t_{\text{TT}}|, \quad (\text{B3})$$

implying a critical value of $V_{\text{EX-TT}} = 2|t_{\text{TT}}|$.

Figure 10 illustrates the solutions when $|t_{\text{EX}}| = |t_{\text{TT}}| = 1$ eV and $V_{\text{EX-TT}} = 3$ eV. At resonance [i.e., $\Delta E = (E_{\text{EX}} - E_{\text{TT}}) = 0$], the $2A_g$ state consists of an equal mixture of bound triplet pairs and bound electron-holes pairs. The mean triplet-triplet separation and electron-hole separation is ca. two dimers. The energy gap between this state and the bands of free triplets and electron holes (i.e., Δ_{2A_g}) is $|t_{\text{TT}}|/3$, in agreement with Eq. (B3). At resonance this energy gap corresponds to the binding energies of both the triplet pairs and electron-hole pairs, i.e., $\Delta_{2A_g} = \Delta_{\text{TT}} = \Delta_{\text{EX}}$.

As the energy of the band of electron-hole excitations increases, i.e., as E_{EX} increases, the system goes off resonance and the $2A_g$ state is predominately composed of bound triplet pairs; the triplet-pair binding energy decreases and the mean triplet-pair separation increases. At a critical value of ΔE , namely, $\Delta E_{\text{critical}}^{\text{U}} = 1.35$ eV, there is a decoupling of the

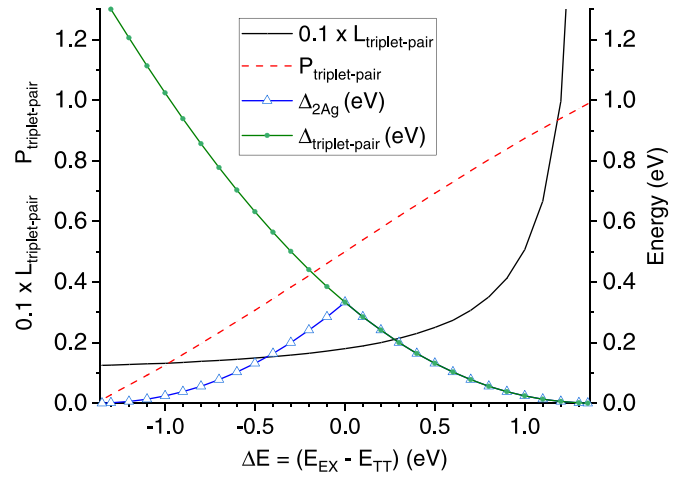


FIG. 10. Non-Coulombically interacting electron-hole pairs (i.e., $\tilde{V} = 0$). $\Delta_{\text{triplet-pair}} = \Delta_{2A_g}$ when $\Delta E \geq 0$. $t_{\text{TT}} = -t_{\text{EX}} = -1.0$ eV, $V_{\text{EX-TT}} = 3.0$ eV. $\Delta E_{\text{critical}} = \pm 1.35$ eV, above and below which the triplet-pair and electron-hole pair subspaces are decoupled. Periodic boundary conditions and 1000 dimers.

triplet-pair and electron-hole pair subspaces: the triplet pair unbinds and the triplet-pair separation diverges. For $\Delta E \geq \Delta E_{\text{critical}}^{\text{U}}$, $P_{\text{triplet-pair}} = 1$.

Similarly, as E_{EX} decreases from resonance the $2A_g$ state is predominately composed of bound electron-hole pairs. Now the triplet-pair binding energy Δ_{TT} increases and the mean triplet-pair separation decreases. Again, there is critical value of ΔE , namely, $\Delta E_{\text{critical}}^{\text{L}} = -1.35$ eV, below which there is a decoupling of the triplet-pair and electron-hole pair subspaces, and the electron-hole pair becomes unbound. For $\Delta E \leq \Delta E_{\text{critical}}^{\text{L}}$, $P_{\text{triplet-pair}} = 0$.

We now turn to the physical limit of interacting electron-hole pairs, i.e., we set the Coulomb interaction $\tilde{V}_{(j-i)} > 0$ in Eq. (16), giving a singlet charge-transfer exciton binding energy of 0.74 eV. As illustrated in Fig. 11, the

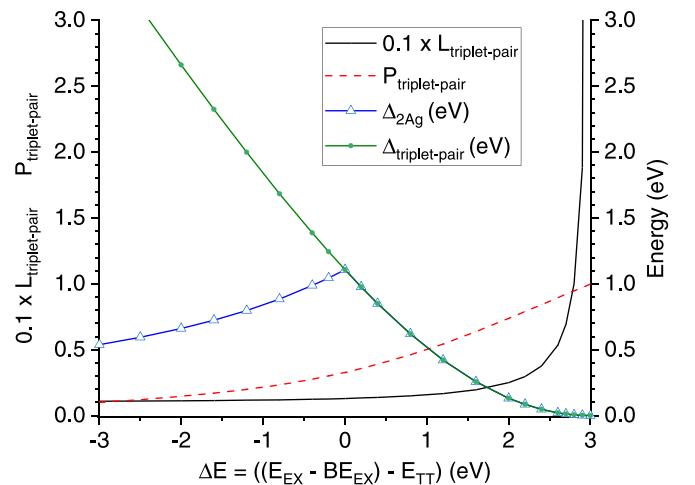


FIG. 11. Coulombically interacting electron-hole pairs (i.e., $\tilde{V} > 0$). $t_{\text{TT}} = -t_{\text{EX}} = -1.0$ eV, $V_{\text{EX-TT}} = 3.0$ eV. $\Delta E_{\text{critical}} = +3.0$ eV above which the triplet-pair and electron-hole pair subspaces are decoupled. The singlet-exciton binding energy, $BE_{\text{EX}} = 0.74$ eV.

electron-hole pair attraction causes a number of significant changes to the $\tilde{V}_{(j-i)} = 0$ picture. As for Fig. 10, the results shown are for $|t_{\text{EX}}| = |t_{\text{TT}}| = 1$ eV and $V_{\text{EX-TT}} = 3$ eV. At resonance the triplet-pair and singlet exciton are mutually stabilized by 1.01 eV. As 1.01 eV is the excitation energy to the free triplet-pair band, this is also the triplet-pair binding energy. This value is considerably enhanced over the $\tilde{V}_{(j-i)} = 0$ limit of 0.333 eV, as the triplets are “slaved” to the Coulombically bound electron-hole pair. We also note that the triplet-pair contribution is only 33%, compared to 50% at resonance in the absence of Coulombically bound electron-hole pairs. Again, as E_{EX} is increased, the triplet-pair binding energy decreases, while the triplet-pair separation and

fraction increases. Above a critical value of E_{EX} , given by $\Delta E \gtrsim 3.0$ eV, there is a decoupling of the triplet-pair and electron-hole subspaces and the triplet-pair unbinds. In contrast, as E_{EX} is decreased there is no such decoupling of the triplet-pair and electron-hole subspaces. In this case the triplet pair becomes more tightly bound, albeit its contribution to the $2A_g$ state becomes less than 10% for $\Delta E < -3.0$ eV.

Figure 11 qualitatively resembles Fig. 7, because $(E_{\text{EX}} - E_{\text{TT}}) = (U - 2t_d)$, so as U is increased the triplet-pair band becomes more stable relative to the singlet exciton. However, $L_{\text{triplet-pair}}$ does not diverge in Fig. 7 when the triplet-pair and exciton subspaces decouple, as that calculation was performed on linear polyene chains of 20 dimers.

- [1] B. S. Hudson and B. E. Kohler, Low-lying weak transition in polyene alpha, omega-diphenyloctatetraene, *Chem. Phys. Lett.* **14**, 299 (1972).
- [2] K. Schulten and M. Karplus, Origin of a low-lying forbidden transition in polyenes and related molecules, *Chem. Phys. Lett.* **14**, 305 (1972).
- [3] W. Barford, *Electronic and Optical Properties of Conjugated Polymers*, 2nd ed. (Oxford University Press, Oxford, 2013).
- [4] P. Tavan and K. Schulten, Electronic excitations in finite and infinite polyenes, *Phys. Rev. B* **36**, 4337 (1987).
- [5] M. Chandross, Y. Shimoi, and S. Mazumdar, Diagrammatic exciton-basis valence-bond theory of linear polyenes, *Phys. Rev. B* **59**, 4822 (1999).
- [6] G. W. Hayden and E. J. Mele, Correlation effects and excited-states in conjugated polymers, *Phys. Rev. B* **34**, 5484 (1986).
- [7] R. J. Bursill and W. Barford, Electron-Lattice Relaxation, and Soliton Structures and Their Interactions in Polyenes, *Phys. Rev. Lett.* **82**, 1514 (1999).
- [8] W. Barford, R. J. Bursill, and M. Y. Lavrentiev, Density-matrix renormalization-group calculations of excited states of linear polyenes, *Phys. Rev. B* **63**, 195108 (2001).
- [9] Y. Ooshika, A semi-empirical theory of the conjugated systems, 2. Bond alternation in conjugated chains, *J. Phys. Soc. Jpn.* **12**, 1246 (1957).
- [10] H. C. Longuet-Higgins and L. Salem, The alternation of bond lengths in long conjugated chain molecules, *Proc. R. Soc. London, Ser. A: Math. Phys. Sci.* **251**, 172 (1959).
- [11] J. A. Pople and S. H. Walmsley, Bond alternation defects in long polyene molecules, *Mol. Phys.* **5**, 15 (1962).
- [12] G. S. Uhrig and H. J. Schulz, Magnetic excitation spectrum of dimerized antiferromagnetic chains, *Phys. Rev. B* **54**, R9624 (1996).
- [13] D. J. Valentine, D. Manawadu, and W. Barford, Higher-energy triplet-pair states in polyenes and their role in intramolecular singlet fission, *Phys. Rev. B* **102**, 125107 (2020).
- [14] Z. G. Soos, S. Ramasesha, and D. S. Galvão, Band to Correlated Crossover in Alternating Hubbard and Pariser-Parr-Pople Chains: Nature of the Lowest Singlet Excitation of Conjugated Polymers, *Phys. Rev. Lett.* **71**, 1609 (1993).
- [15] D. Mukhopadhyay, G. W. Hayden, and Z. G. Soos, Molecular-exciton approach to spin-charge crossovers in dimerized Hubbard and excitonic chains, *Phys. Rev. B* **51**, 9476 (1995).
- [16] M. Yu. Lavrentiev and W. Barford, $1^1B_u^- - 2^1A_g^+$ crossover in conjugated polymers: The phase diagram of the molecular-orbital model, *Phys. Rev. B* **59**, 15048 (1999).
- [17] B. Kraabel, D. Hulin, C. Aslangul, C. Lapersonne-Meyer, and M. Schott, Triplet exciton generation, transport and relaxation in isolated polydiacetylene chains: Subpicosecond pump-probe experiments, *Chem. Phys.* **227**, 83 (1998).
- [18] G. Lanzani, S. Stagira, G. Cerullo, S. De Silvestri, D. Comoretto, I. Moggio, C. Cuniberti, G. F. Musso, and G. Dellepiane, Triplet exciton generation and decay in a red polydiacetylene studied by femtosecond spectroscopy, *Chem. Phys. Lett.* **313**, 525 (1999).
- [19] A. J. Musser, M. Al-Hashimi, M. Maiuri, D. Brida, M. Heeney, G. Cerullo, R. H. Friend, and J. Clark, Activated singlet exciton fission in a semiconducting polymer, *J. Am. Chem. Soc.* **135**, 12747 (2013).
- [20] Y. Kasai, Y. Tamai, H. Ohkita, H. Benten, and S. Ito, Ultrafast singlet fission in a push-pull low-bandgap polymer film, *J. Am. Chem. Soc.* **137**, 15980 (2015).
- [21] D. Manawadu, D. J. Valentine, M. Marcus, and W. Barford, Singlet triplet-pair production and possible singlet-fission in carotenoids, *J. Phys. Chem. Lett.* **13**, 1344 (2022).
- [22] T. Polivka and V. Sundström, Ultrafast dynamics of carotenoid excited states — From solution to natural and artificial systems, *Chem. Rev.* **104**, 2021 (2004).
- [23] H. Hashimoto, C. Urugami, N. Yukihiro, A. T. Gardiner, and R. J. Cogdell, Understanding/unravelling carotenoid excited singlet states, *J. R. Soc., Interface* **15**, 20180026 (2018).
- [24] A. J. Musser and J. Clark, Triplet-pair states in organic semiconductors, *Annu. Rev. Phys. Chem.* **70**, 323 (2019).
- [25] W. F. Hu and G. K. L. Chan, Excited-state geometry optimization with the density matrix renormalization group, as applied to polyenes, *J. Chem. Theory Comput.* **11**, 3000 (2015).
- [26] E. J. Taffet, B. G. Lee, Z. S. D. Toa, N. Pace, G. Rumbles, J. Southall, R. J. Cogdell, and G. D. Scholes, Carotenoid nuclear reorganization and interplay of bright and dark excited states, *J. Phys. Chem. B* **123**, 8628 (2019).
- [27] D. Khokhlov and A. Belov, Ab initio study of low-lying excited states of carotenoid-derived polyenes, *J. Phys. Chem. A* **124**, 5790 (2020).
- [28] W. Barford, R. J. Bursill, and M. Y. Lavrentiev, Density matrix renormalization group calculations of the low-lying excitations

- and non-linear optical properties of poly(para-phenylene), *J. Phys.: Condens. Matter* **10**, 6429 (1998).
- [29] A. B. Harris, Alternating linear Heisenberg antiferromagnet-exciton limit, *Phys. Rev. B* **7**, 3166 (1973).
- [30] W. H. Zheng, C. J. Hamer, R. R. P. Singh, S. Trebst, and H. Monien, Deconfinement transition and bound states in frustrated Heisenberg chains: Regimes of forced and spontaneous dimerization, *Phys. Rev. B* **63**, 144411 (2001).
- [31] E. J. Taffet, D. Beljonne, and G. D. Scholes, Overlap-driven splitting of triplet pairs in singlet fission, *J. Am. Chem. Soc.* **142**, 20040 (2020).
- [32] M. Chandross and S. Mazumdar, Coulomb interactions and linear, nonlinear, and triplet absorption in poly(para-phenylenevinylene), *Phys. Rev. B* **55**, 1497 (1997).
- [33] W. Barford, R. J. Bursill, and R. W. Smith, Theoretical and computational studies of excitons in conjugated polymers, *Phys. Rev. B* **66**, 115205 (2002).
- [34] The even-parity excitons alternate in energy with the odd-parity excitons, while the lowest even-parity (Frenkel) exciton is split off from the Rydberg series [3,33].
- [35] D. C. Mattis, *The Theory of Magnetism*, 1st ed. (Springer-Verlag, Berlin, 1988), p. 147.
- [36] F. B. Gallagher and S. Mazumdar, Excitons and optical absorption in one-dimensional extended Hubbard models with short- and long-range interactions, *Phys. Rev. B* **56**, 15025 (1997).
- [37] F. Gebhard, K. Bott, M. Scheidler, P. Thomas, and S. W. Koch, Exact results for the optical absorption of strongly correlated electrons in a half-filled Peierls-distorted chain, *Philos. Mag. B* **75**, 13 (1997).